Polyolefin blends: effect of EPDM rubber on crystallization, morphology and mechanical properties of polypropylene/EPDM blends. 1

V. Choudhary, H. S. Varma and I. K. Varma
Centre for Materials Science and Technology, Indian Institute of Technology Delhi, Hauz Khas, New Delhi 110016, India
(Received 29 May 1990; revised 18 July 1990; accepted 22 August 1990)

Morphology, thermal behaviour and mechanical and dynamic mechanical properties of isotactic polypropylene (PP) blended with different amounts of ethylene–propylene–diene (EPDM) terpolymer were investigated. Addition of 10% (w/w) EPDM to PP resulted in an increase in spherulite size. Optical micrographs showed that the rubber was distributed both in the intra- and interspherulitic regions. The heat of fusion (ΔH_f) and percentage crystallinity (wide angle X-ray scattering) of PP/EPDM blends decreased on increasing EPDM content. Scanning electron micrographs revealed a skin–core morphology in injection-moulded specimens. Melt viscosity of the PP/EPDM blends determined at 200°C using a capillary rheometer showed an increase with increasing rubber content. A non-Newtonian flow behaviour was observed in the shear rate range 40–1600 s^{-1}. Dynamic mechanical analysis results also supported the incompatibility of PP/EPDM blends. An improvement in impact strength of PP was observed upon incorporation of EPDM elastomer.

(Keywords: polyolefin blends; crystallization; morphology; mechanical properties)

INTRODUCTION

Considerable work has been carried out to improve the impact strength of polypropylene (PP) by incorporation of elastomers. The elastomers investigated include ethylene–propylene copolymer[1–3], butyl rubber and the styrene–butadiene–styrene system[4,5]. The effect of composition of ethylene–propylene rubber on the blend properties and morphology has been evaluated[6]. However, very few publications[7–10] deal with the effect of ethylene–propylene–diene (EPDM) terpolymer content on the morphology and properties of PP/EPDM blends.

Earlier we reported[11,12] the effect of EPDM content on the crystallization and morphology of high density polyethylene (HDPE) and a binary blend of PP/HDPE (90/10). We now report the morphology, thermal and mechanical and dynamic mechanical properties of binary PP/EPDM blends of varying composition.

EXPERIMENTAL

Materials

Isotactic PP (Koylene M3030) was obtained from the Indian Petrochemical Corporation Ltd (melt flow index 3.0 g per 10 min) and EPDM (NORDEL 2760) was obtained from DuPont. The ethylene (C_2) content of EPDM rubber, as determined by Fourier transform infra-red spectroscopy (ASTM D 3900), was found to be ~80 wt% with a small amount of 1,4-hexadiene.

Preparation of blends

A Betol single screw extruder (length/diameter = 19.47) was used for melt blending the polymers. The granules of PP and EPDM were hand mixed in appropriate ratios prior to being added to the extruder hopper. The temperatures of the four zones of the extruder were: feed zone 190°C; compression zone 200°C; metering zone 210°C; and die zone 210°C. The screw speed was adjusted to 20 rev min^{-1}. The filament obtained upon extrusion was immediately quenched in water and later chopped into small granules. The unblended PP was also subjected to the same extrusion process in order to obtain a similar thermal history to that of the PP component in the binary PP/EPDM blends.

Various binary blends were prepared by varying the rubber content from 0 to 30% (w/w). The samples are designated PPB_5, PPB_{10}, PPB_{15}, PPB_{20}, PPB_{25} and PPB_{30} where B stands for the EPDM rubber and the subscript indicates the weight per cent of rubber in the blends.

Measurements

A DuPont 1090 thermal analyser with a 910 differential scanning calorimetry (d.s.c.) module was used for recording d.s.c. scans in a static air atmosphere. A sample size of 10 ± 1 mg was used in each experiment. The polymer sample in the powdered form was heated to 180°C and was maintained at this temperature for 5 min to allow all the crystallites to melt. In the cooling cycle, the sample was cooled from 180 to 30°C under a controlled cooling rate of 10°C min^{-1}. The samples were maintained at this temperature for 10 min and then heated to 180°C at a heating rate of 10°C min^{-1} (heating cycle).

Wide angle X-ray diffraction measurements on the various blend samples were performed using a Phillips X-ray generator equipped with a microprocessor-controlled recorder unit. Radial scans of intensity *versus*

0032-3861/91/142534-07

diffraction angle, 2θ, were recorded in the range 10–50° for 2θ under identical settings using nickel-filtered CuKα radiation of wavelength 1.5418 Å. An operating voltage of 40 kV and filament current of 30 mA were used.

The shape, size and nucleation density of spherulites in the various samples was investigated using a Lietz Laborlux 12 POL polarizing microscope. For this study, thin polymer films ($\sim 50\ \mu m$) were prepared by compression moulding using a Carver laboratory press at a temperature of 200°C and a pressure of $\sim 560\ kg\ cm^{-2}$. The polymer films were then taken out of the press and cooled to room temperature. Annealing was carried out by heating the films between two cover slips in a silicone oil bath maintained at 175°C for ~5 min and subsequent cooling at an isothermal crystallization temperature (T_c) of 120°C for 0.5, 1, 2, 5, 10, 20 and 30 min. After completion of each isothermal crystallization, the polymer films were quench cooled in an ice–water mixture to freeze the morphology. These films were then micrographed.

Polymer granules obtained after blending were dried at 70°C for 4 h and then stored in plastic bags in a desiccator over anhydrous $CaCl_2$. These granules were then used for melt rheology studies. Flow behaviour of PP and PPB blends at 200°C was investigated using a MCR capillary (length/diameter = 20) rheometer attached to an Instron model 1112. The true shear rate at the wall ($\dot{\gamma}_w$), true shear stress at the wall (τ_w) and melt viscosity were calculated using standard procedures[13].

Dumb-bell shaped specimens for tensile testing were prepared by a SP 1 Windsor injection moulding machine at an injection temperature of 200°C and an injection pressure of $120\ kg\ cm^{-2}$. Tensile (ASTM D-638) and impact properties (ASTM D-256) of injection-moulded samples were investigated using an Instron tensile tester (Model 1121) and Izod impact tester (model IT-0.42) at 25°C and 65% relative humidity, respectively. A cross-head speed of $20\ mm\ min^{-1}$, chart drive of $20\ mm\ min^{-1}$, full scale load of 200 kg and jaw separation of 50 mm were used for tensile testing.

Dynamic mechanical measurements on various polymer samples were carried out in the temperature range −100°C to 100°C using a DuPont 1090 thermal analyser having a 982 dynamic mechanical analysis (d.m.a.) module. Samples for d.m.a. studies were cut from the injection-moulded dumb-bell shaped tensile specimens. The length to thickness ratio was kept at 10.

Scanning electron micrographs of cryogenically fractured notched impact specimens were recorded on a Cambridge S4-10 stereoscan microscope. Notched impact specimens of PPB blends were frozen in liquid nitrogen for 1 h, placed in a frame and quickly fractured in the impact mode. Fractured surfaces were then etched in cyclohexane for 1 h at room temperature and subsequently sprayed with fresh cyclohexane to remove EPDM inclusions. These samples were then mounted on a base plate and coated with silver using vapour deposition techniques prior to scanning.

RESULTS AND DISCUSSION

Crystallization exotherms were observed during the cooling cycle in the d.s.c. scan for PP and binary PPB blends in the temperature range 128–100°C. Crystallization exotherms were characterized by determining:

1. the peak temperature of the crystallization exotherm (T_c);
2. the temperature of onset of crystallization (T_{onset}), which is the temperature where the thermogram initially departs from the baseline on the high temperature side of the exotherm;
3. the heat of crystallization (ΔH_0), determined from the area under the exotherm.

Addition of increasing concentration of EPDM rubber to PP resulted in a decrease in T_c of PP (119.3°C), and in PPB_{30} blend T_c was observed at 115.8°C. Similarly ΔH_0 and T_{onset} decreased on addition of EPDM to PP. The compositional dependence of T_c, relative T_{onset} (i.e. T_{onset} blend/T_{onset} PP) and ΔH_0 in PPB blends is shown in *Figure 1*. A decrease in T_{onset} in the PPB blends clearly indicates that the inclusion of a rubbery phase in PP results in delayed nucleation. However, if the difference between T_{onset} and T_c is examined, a significant reduction (~2.6°C) is obtained by addition of 5% EPDM. Such a decrease can be attributed to an increase in the rate of crystallization. The difference in T_{onset} and T_c values was lower than for PP but higher than for the PPB_5 blend when the concentration of EPDM was increased to ~30%. The increased rate of crystallization in the presence of EPDM may be due to the enhanced mobility of the PP segments thereby leading to better alignment in the crystal lattice.

The observed decrease in ΔH_0 values can be explained due to the presence of rubber which acts as a diluent. No change in ΔH_0 is observed compared to PP on subtracting the weight per cent of rubber in the PPB blends and recalculating ΔH_0 only on the weight per cent of PP component. These results thus indicate that the propylene/ethylene segments of EPDM do not co-crystallize with PP. If such a crystallization had taken place then ΔH_0 for the blend would have become higher. Since the ΔH_0 value for the PP component remains unchanged in PPB blends, it can therefore be concluded that EPDM does not act as an inhibitor for PP crystallization.

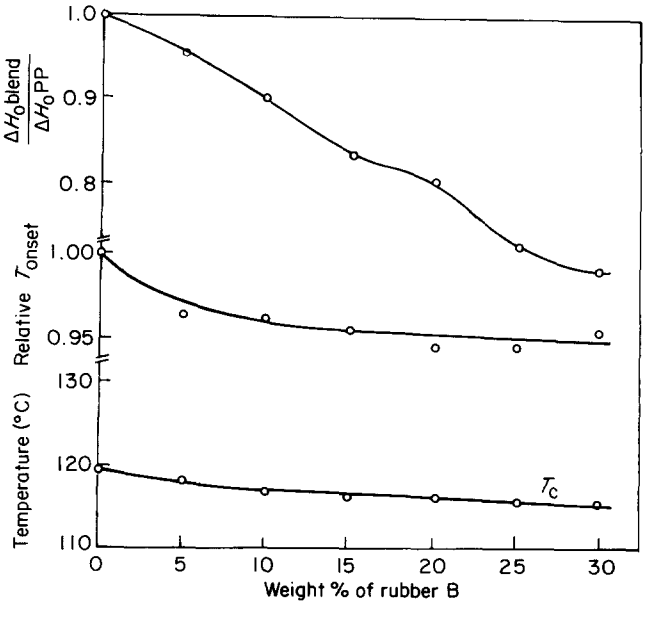

Figure 1 Effect of EPDM rubber on the crystallization parameters of PP in PPB blends

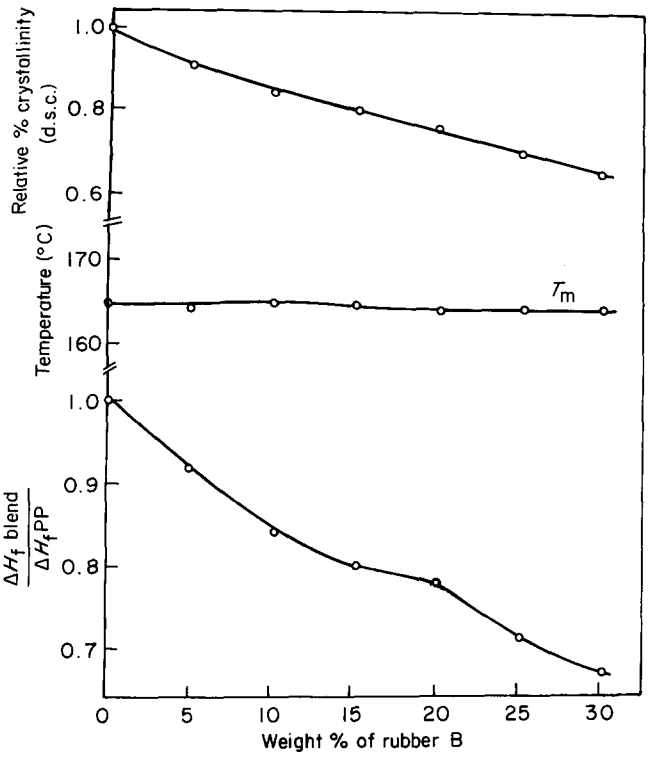

Figure 2 Effect of EPDM rubber on the melting transition of PP in PPB blends

The melting temperature(T_m), heat of fusion (ΔH_f) and width at half-height of the fusion peak were determined from the heating cycle of a d.s.c. scan. The percentage crystallinity was also calculated by using the relationship:

$$\% \text{ crystallinity} = \frac{\Delta H_f^{obs}}{\Delta H_f^0} \times 100$$

A value of ΔH_f^0 of 209 J g^{-1} for 100% crystalline PP homopolymer was used for calculating the percentage crystallinity[6].

The effect of EPDM rubber on the phase transition of PP in PPB blends is shown in *Figure 2*. A marginal change in T_m of PP was observed on addition of EPDM rubber from 5 to 30%. In conformity with heat of crystallization (ΔH_0), heat of fusion and percentage crystallinity decreased with increasing EPDM rubber content. The width at half-height of the fusion peak increased to some extent on addition of EPDM rubber thus indicating an increase in heterogeneity in the spherulite size.

X-ray diffraction studies of PP and PPB blends showed peaks at 2θ of 14.0, 17.0, 18.5 and 21.3° corresponding to the (1 1 0), (0 4 0), (1 3 0), (1 1 1) and (1 3 1) diffraction peaks (*Figure 3*). Similar crystalline peaks have earlier been reported by Natta and Corrdani[14] for PP. The presence of these characteristic crystalline peaks of PP in PPB blends clearly indicates that the crystal structure of PP remains unchanged upon addition of different weight percentages of EPDM. The *d* spacings were also calculated from these *hkl* values and were found to be 6.30, 5.20, 4.80, 4.10 and 3.63 Å, respectively.

However the intensities of the peaks decreased especially at *hkl* (1 1 0), (0 4 0) and (1 3 0), indicating that by incorporation of EPDM, the proportion of the monoclinic (α form) and hexagonal (β form) phases are modified in the PP matrix. This variation in the peak heights could be due to the variation of the mean spherulite size or their distribution, deformation at the spherulite boundaries or any long range order induced in the structure by the dispersion of EPDM domains in the PP matrix.

The degree of crystallinity (X_c) was calculated from the diffractograms by the method reported in the literature[15]:

$$X_c = \frac{\int_0^\infty S^2 I_{cr}(S)\, ds}{\int_0^\infty S^2 I(S)\, ds} K$$

where $I_{cr}(S)$ is the coherent intensity concentrated in the crystalline peaks, $I(S)$ is the total coherent intensity

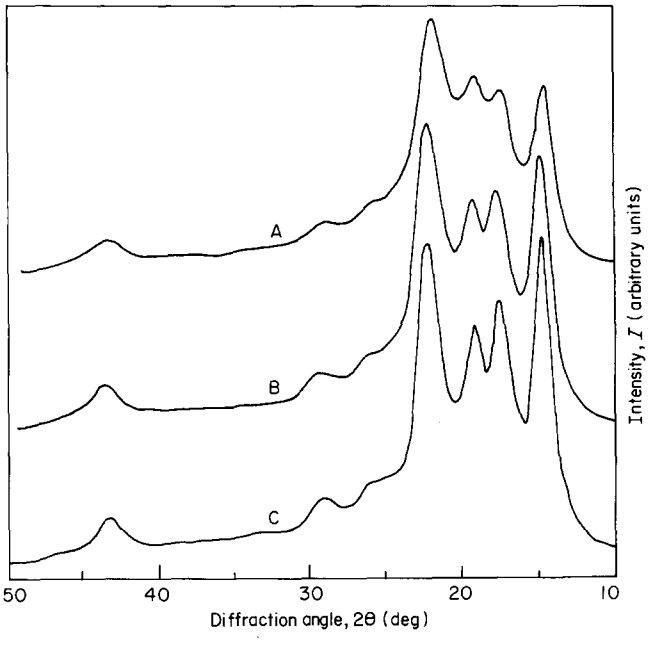

Figure 3 *I versus* 2θ plots of: (A) PPB_{30}; (B) PPB_{15}; (C) PPB_5

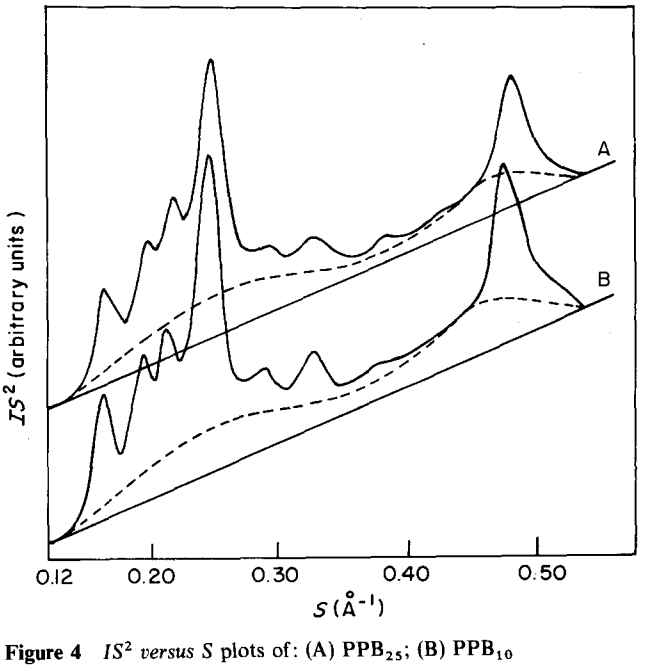

Figure 4 IS^2 *versus* S plots of: (A) PPB_{25}; (B) PPB_{10}

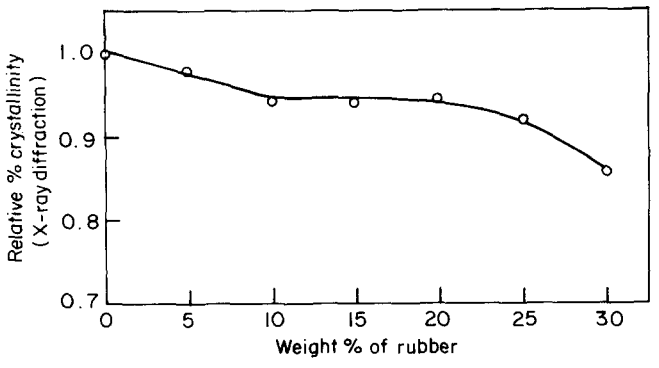

Figure 5 Effect of blend composition on percentage crystallinity in PPB blends

scattered, S is the scattering vector expressed as $S = (2/\lambda) \sin \theta$, and K is the correction factor, which depends on the atomic scattering factor and the disorder function[15,16]. Owing to the uncertainty of the value of the disorder function, this factor was ignored in these calculations by taking the K value to be equal to unity. The degree of crystallinity thus evaluated is denoted as apparent degree of crystallinity (X_c) which is emphasized for its comparative value alone.

The experimental I *versus* 2θ curves were converted into IS^2 *versus* S curves (*Figure 4*). The baseline and amorphous curve were drawn in accordance with the method reported earlier[15]. The percentage apparent

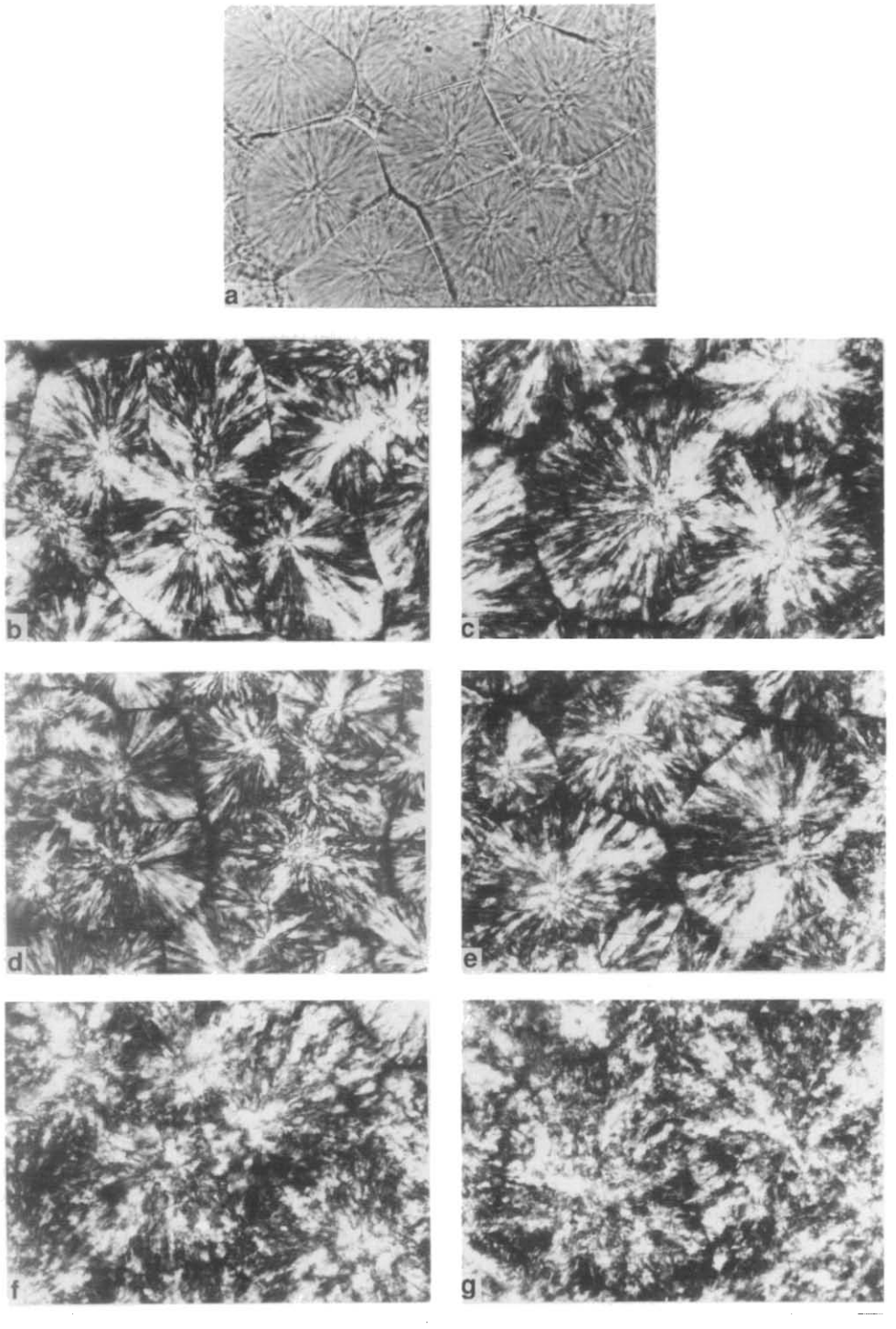

Figure 6 Optical micrographs of PP and various binary PPB blends obtained after annealing at 120°C for 20 min. (a) PP; (b) PPB_5; (c) PPB_{10}; (d) PPB_{15}; (e) PPB_{20}; (f) PPB_{25}; (g) PPB_{30}

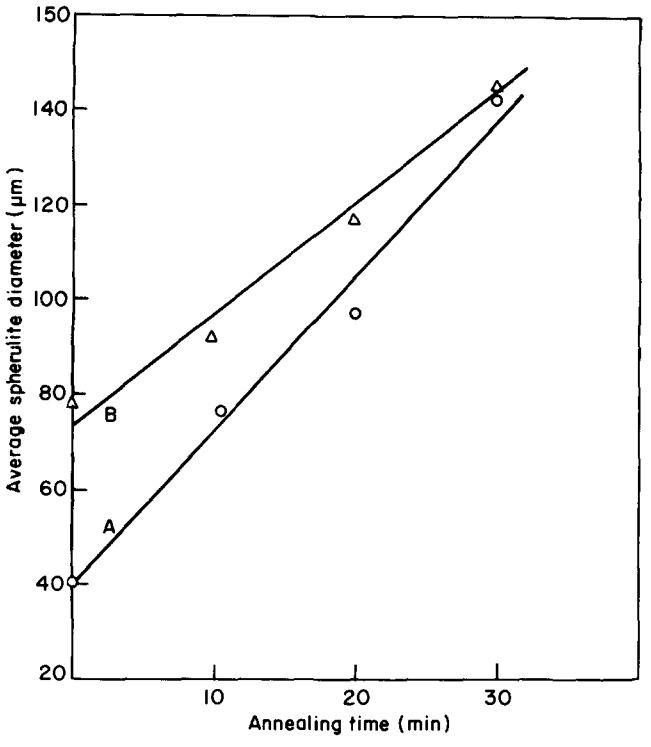

Figure 7 Effect of annealing time on spherulite size in (A) PP and (B) PPB binary blends

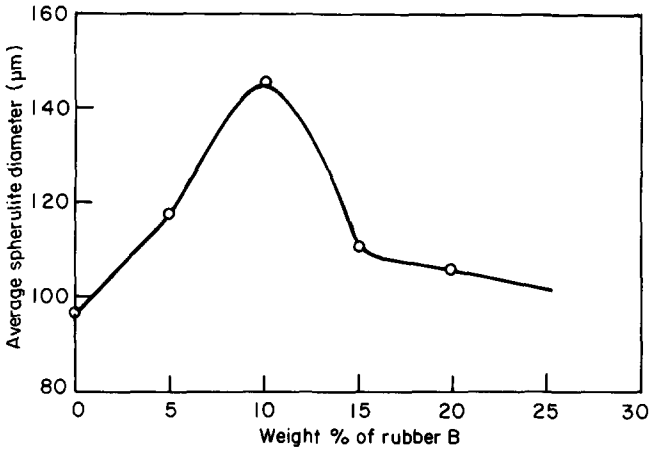

Figure 8 Effect of blend composition on average spherulite size of PP in PPB blends (annealing at 120°C for 20 min)

degree of crystallinity was found to decrease on increasing the EPDM content in PPB blends (*Figure 5*).

The effect of blend composition on the spherulite size of PP after annealing at 120°C for 20 min is shown in *Figure 6*. Spherulitic boundaries were not clear in the PPB_{25} and PPB_{30} binary blends. The rate of spherulitic growth in various PPB blends was also investigated at an annealing temperature of 120°C using optical microscopy. The size of PP spherulites in PP and PPB blends increased with increase in annealing time from 0 to 30 min (*Figure 7*). Spherulite size of PP increased on addition of EPDM rubber up to ~10% followed by a decrease (*Figure 8*). These results indicate that addition of elastomer up to ~10% affects the rate of crystallization thereby leading to the formation of larger spherulites. These results thus provide support for the d.s.c. observation.

Flow behaviour

A non-Newtonian flow behaviour was observed in all binary blends. Addition of EPDM rubber resulted in an increase in melt viscosity of PP at all compositions (*Figure 9*). The variation in melt viscosity also depended on the shear stress. Theoretical values of viscosity were calculated for various blends using the log additivity principle[17] and the values are given in *Table 1*. The calculated values of melt viscosity of PPB blends were higher than the experimental values (*Table 1*) and the

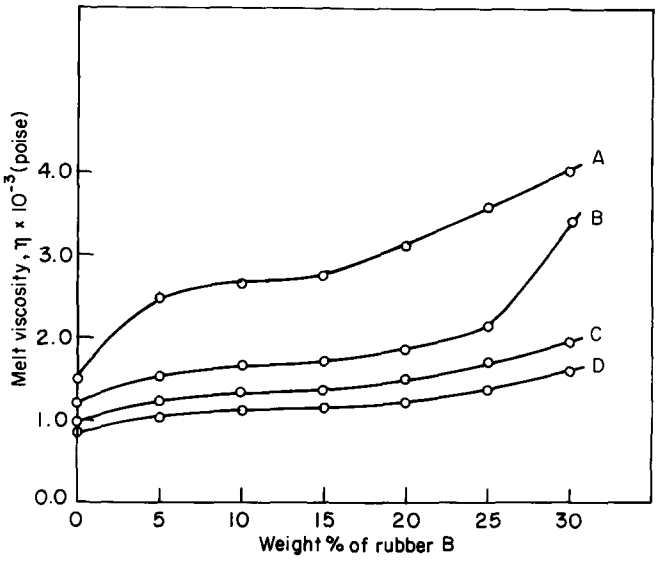

Figure 9 Composition dependence of melt viscosity, η, of PPB blends at 200°C and length/diameter = 20. The shear stress, τ_w, is: (A) 14×10^4; (B) 18×10^4; (C) 20×10^4; (D) 22×10^4 N m^{-2}

Table 1 Values of melt viscosity of PP, rubber B and binary PPB blends at 200°C and length/diameter = 20

Sample designation	Shear stress, τ_w ($\times 10^{-4}$) (N m^{-2})	Melt viscosity, η ($\times 10^{-3}$) (poise)	Power law exponent, n	Theoretical viscosity $\ln \eta_b = \sum w_i \ln \eta_i$
PP	14	1.50	0.37	–
	20	0.95		–
	22	0.75		–
PPB_5	14	2.50	0.33	4.92
	20	1.22		3.30
	22	1.02		2.91
PPB_{10}	14	2.65	0.34	8.35
	20	1.32		5.65
	22	1.10		5.07
PPB_{15}	14	2.76	0.33	11.77
	20	1.36		8.00
	22	1.14		7.23
PPB_{20}	14	3.10	0.33	15.20
	20	1.50		10.36
	22	1.25		9.40
PPB_{25}	14	3.60	0.34	18.62
	20	1.70		12.71
	22	1.40		11.56
PPB_{30}	14	4.00	0.32	22.05
	20	1.94		15.06
	22	1.59		13.72
B	14	70.00	–	–
	20	48.00		–
	22	44.00		–

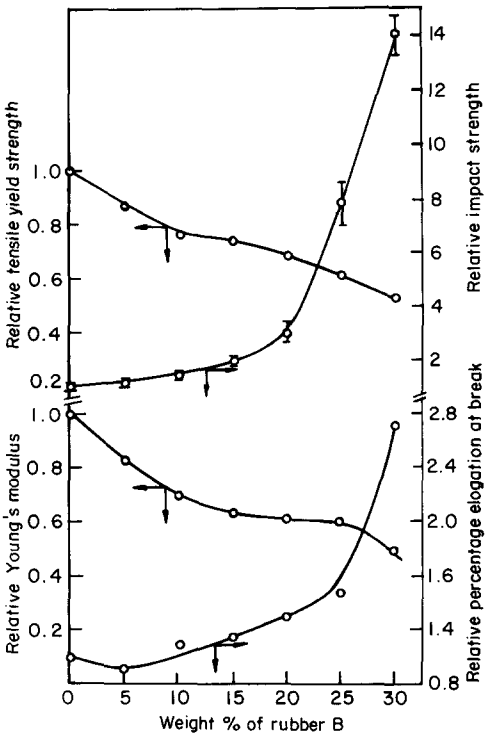

Figure 10 Effect of blend composition on the mechanical properties of PPB blends

deviation increased as the rubber concentration was increased from 5 to 30%.

A linear relationship was observed between shear stress (τ_w) and shear rate ($\dot{\gamma}_a$). The values of the power law exponent (n) of PP and PPB blends varies from 0.32 to 0.37 indicating pseudoplastic behaviour. The blend composition had an insignificant effect on the value of n (*Table 1*).

The melt fracture or extrudate distortion is important in polymer processing to achieve acceptable product quality. Effect of shear stress on extrudate distortion was studied in PPB_{10} at 200°C (length/diameter = 20). Extrudate distortion started appearing at a shear stress of $\sim 16 \times 10^4$ N m^{-2} and increased on further increase in shear stress.

Tensile and impact properties

Figure 10 shows the effect of blend composition on the tensile and impact properties of PP. The tensile strength at yield and Young's modulus decreased with increasing rubber content. A marginal decrease in percentage elongation at break was observed upon incorporation of 5% (w/w) of EPDM rubber. At higher concentrations of rubber the percentage elongation at break increased. Incorporation of rubber in PP resulted in a significant improvement in the impact strength of the binary blends. Addition of 30% (w/w) EPDM rubber to PP resulted in a ~14-fold (~1333%) increase in impact strength when compared to PP (*Figure 10*).

Dynamic mechanical analysis

The temperature dependence of the loss and storage moduli of PPB blends are shown in *Figure 11*. Pure PP and EPDM homopolymers had glass transition temperature (T_g) values at 25 and −24°C, respectively. In PPB_{10}, a broad maximum at −33°C and another sharp loss modulus maximum at 24°C were present. As the rubber content was increased from 10 to 20% (w/w), two well defined loss modulus maxima were observed at −40 and 23°C, respectively. The PPB_{30} blend had two T_g maxima at −34 and +23°C, corresponding to rubber and PP phases present in the system.

The T_g values in partially compatible blends are expected to shift towards each other[18]. However, in the blends under investigation the T_g of PP remains unaffected by the presence of EPDM rubber. The T_g of EPDM rubber however shifted to lower temperatures, i.e. from −24 for pure EPDM to −34°C for PPB_{30}. A depression in T_g of rubber particles has been observed in several multicomponent systems[10,19,20]. Rubber inclusions have a higher thermal expansion coefficient than the PP matrix. Cooling of blend from the melt thus results in a negative hydrostatic pressure acting on rubber particles. Thermal stresses thus generated may be responsible for the observed decrease in T_g of EPDM in PPB blends.

Scanning electron microscopy

Scanning electron micrographs (*Figure 12*) of cryogenically impact-fractured specimens revealed that the addition of rubber to PP resulted in a skin–core morphology. Elongated rubbery inclusions due to the elongational flow at the wall were observed in the subsurface layer whereas the skin consisted of a thin pure PP layer. The mould filling process of an injection-moulded polymer blend can be best described in terms of the 'fountain flow' theory first proposed by Rose[21] and subsequently elaborated by other workers[22,23]. When the polymer melt is injected through the gate from the barrel of the machine into the mould cavity, it

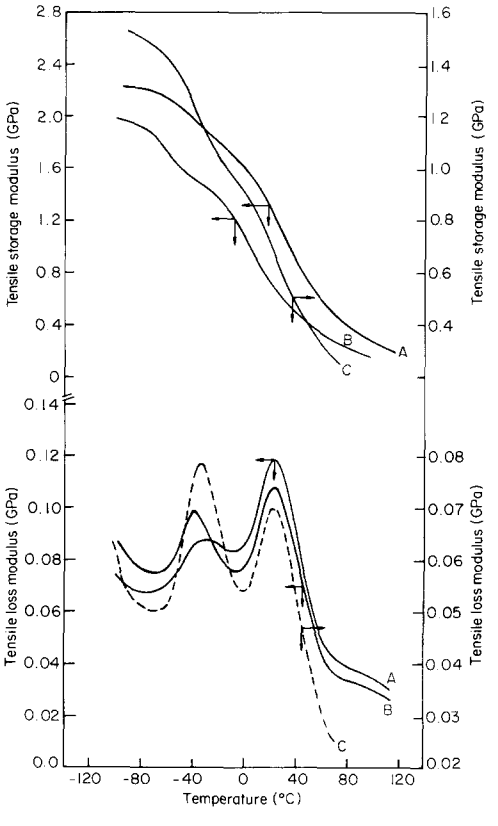

Figure 11 Dynamic mechanical analysis traces of PPB blends: (A) PPB_{10}; (B) PPB_{20}; (C) PPB_{30}

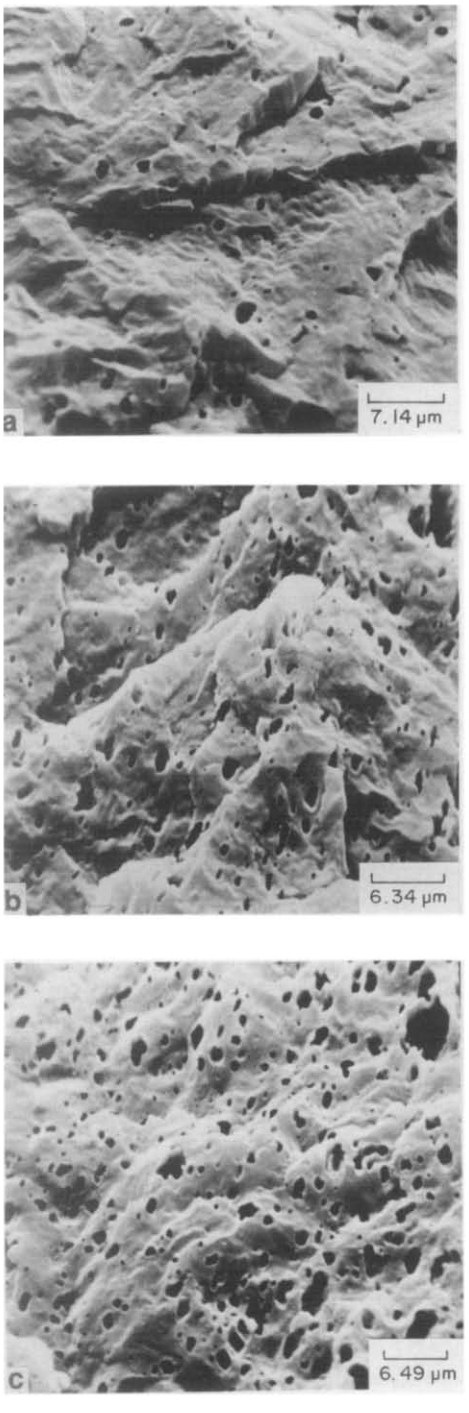

Figure 12 Scanning electron micrographs of injection-moulded PPB blends: (a) PPB_5; (b) PPB_{15}; (c) PPB_{30}

experiences large elongational and compressional fields. The material solidifies at the surface of the mould forming a skin and the mould is then filled by material which flows through the core region to the advancing front. The elongation is created during the stretching flow of the frontal portion of the stream, and subsequently moved to the cold walls and frozen. The deformation of rubbery particles decreased but their concentration increased with increasing distance from the skin towards the core. In the binary PP/EPDM blends, the size and number of rubber particles increased as the concentration of rubber increased up to 30% (w/w).

CONCLUSIONS

The following conclusions can be drawn.

1. PP/EPDM blends at all compositions were found to be incompatible.
2. Differential scanning calorimetry results indicate that addition of EPDM resulted in an increase in the rate of crystallization whereas nucleation is delayed.
3. A decrease in percentage crystallinity on increasing EPDM rubber in PPB blends is observed. On incorporation of EPDM rubber, the proportion of monoclinic (α form) and hexagonal (β form) phases is modified in the PP matrix.
4. EPDM rubber was distributed both in the intra- and interspherulitic region. Spherulite size of PP also increased on addition of 10% (w/w) EPDM. On addition of higher amounts of EPDM (>20%), the spherulitic boundaries were damaged and spherulites were not identifiable from each other.
5. A large improvement in the Izod impact strength of PP occurs on increasing the EPDM rubber content.

REFERENCES

1 Martuscelli, E., Silvestre, S. and Bianchi, L. *Polymer* 1983, **24**, 1458
2 Martuscelli, E., Silvestre, C. and Abate, G. *Polymer* 1982, **23**, 229
3 D'Orazio, L., Greco, R., Martuscelli, E. and Ragosta, G. *Polym. Eng. Sci.* 1983, **23**, 489
4 Plochocki, A. P. in 'Polymer Blends', Ch. 21, Academic Press, New York, 1978
5 Bianchi, L., Cimmino, S., Forte, A., Grew, R., Martuscelli, E., Riva, F. and Silvestre, C. *J. Mater. Sci.* 1985, **20**, 895
6 Greco, R., Mancarella, C., Martuscelli, E., Ragosta, G. and Jinghua, Y. *Polymer* 1987, **28**, 1929
7 Kalfoglou, N. K. *Angew. Makromol. Chem.* 1985, **129**, 103
8 Dao, K. C. *J. Appl. Polym. Sci.* 1982, **27**, 4799
9 Ghang Sik Ha, Dong Joon Ihm and Sung Chul Kim. *J. Appl. Polym. Sci.* 1986, **32**, 6281
10 Kolarik, J., Agrawal, G. L., Krulis, Z. and Kovar, J. *Polym. Comp.* 1986, **7**, 463
11 Choudhary, V., Varma, H. S. and Varma, I. K. *J. Therm. Anal.* 1987, **32**, 579
12 Varma, H. S., Choudhary, V. and Varma, I. K. *J. Therm. Anal.* 1989, **35**, 1257
13 Han, C. D. 'Rheology in Polymer Processing', Ch. 5, Academic Press, New York, 1976
14 Natta, G. and Corrdani, P. *Nuvo Cimento* 1960, **15**, 40
15 Ruland, W. *Acta Crystallogr.* 1961, **14**, 1180
16 Sotton, M., Arniand, A. M. and Rabourdin, C. *Bull. Sci. Inst. Text. Fr.* 1978, **7**, 265
17 Utracki, L. A. *Polym. Eng. Sci.* 1989, **23**, 602
18 McKnight, W. J., Karasz, F. E. and Fried, J. R. in 'Polymer Blends' (Eds D. R. Paul and S. Newman), Academic Press, New York, 1978
19 Bohn, L. *Angew. Makromol. Chem.* 1971, **20**, 129
20 Bates, F. S., Cohen, R. E. and Argon, A. S. *Macromolecules* 1983, **16**, 1108
21 Rose, W. *Nature* 1961, **191**, 242
22 Tadmor, Z. *J. Appl. Polym. Sci.* 1974, **18**, 1753
23 Katti, S. S. and Schultz, J. M. *Polym. Eng. Sci.* 1981, **22**, 1001